

# Differentiated appendages in *Isoxys* illuminate origin of arthropodization

**Caixia Zhang**

Yunnan University

**Yu Liu** (✉ [yu.liu@ynu.edu.cn](mailto:yu.liu@ynu.edu.cn))

Yunnan University <https://orcid.org/0000-0002-2346-740X>

**Javier Ortega-Hernández**

Harvard University <https://orcid.org/0000-0002-6801-7373>

**Joanna Wolfe**

Museum of Comparative Zoology and Department of Organismic and Evolutionary Biology, Harvard University

**Changfei Jin**

Yunnan University

**Huijuan Mai**

Yunnan University

**Xian-guang Hou**

Yunnan Key Laboratory for Palaeobiology

**Jin Guo**

Yunnan University

**Dayou Zhai**

Yunnan University

---

## Biological Sciences - Article

**Keywords:** Cambrian fossil record, euarthropod evolution, Isoxys appendages, arthropodization

**Posted Date:** September 3rd, 2021

**DOI:** <https://doi.org/10.21203/rs.3.rs-861892/v1>

**License:**  This work is licensed under a Creative Commons Attribution 4.0 International License.

[Read Full License](#)

---

# Abstract

The Cambrian fossil record has produced remarkable insights into the origin of euarthropods, particularly the evolution of their versatile body plan of segments bearing specialized, jointed appendages for different functions including feeding and locomotion [01, 02]. Early euarthropod evolution involved a major transition from lobopodian-like taxa [03, 04, 05] to organisms featuring a fully sclerotized trunk (arthrodization) and limbs (arthropodization) [02, 06, 07, 08]. However, the precise origin of arthropodization remains controversial because some of the earliest branching euarthropods possess a broad dorsal carapace that obscures critical details of the trunk and appendage organization [09, 10, 11, 12, 13, 14, 15]. Here, we demonstrate the presence of fully arthropodized ventral appendages in the upper stem-group euarthropod *Isoxys curvirostratus* from the early Cambrian Chengjiang biota in South China. Micro-computed tomography reveals the detailed three-dimensional structure of the biramous appendages in *I. curvirostratus* for the first time. In addition to the raptorial frontal appendages *I. curvirostratus* also possesses two batches of morphologically distinct biramous limbs, with the first batch consisting of four pairs of short cephalic appendages bearing prominent endites with a feeding function, followed by a second batch of elongate trunk appendages for locomotion. Each biramous limb bears an endopod with more than 12 well-defined podomeres, and an exopod consisting of a slender shaft carrying approximately a dozen paddle-shaped lamellae. Our findings clarify the enigmatic appendicular organization of *Isoxys*, one of the most ubiquitous euarthropods in Cambrian Burgess Shale-type deposits worldwide [01, 10, 11, 12, 14, 15, 16, 17, 18]. Critically, our new material shows that the trunk of *I. curvirostratus* was not arthrodized. The phylogenetic position of isoxysiids as possibly the earliest branching members of Deuteropoda [01, 02, 07, 15, 19], suggests that arthropodized biramous appendages evolved before the pattern of full trunk arthrodization that characterizes most extant and extinct members of this successful animal phylum.

# Main Text

The presence of segmented appendages with joints consisting of hardened (sclerotized) cuticle connected by flexible membranes – formally known as arthropodization – represents the most recognizable character of most extant and extinct euarthropods [01, 02, 06, 07, 08, 13, 21]. Arthropodized limbs are enormously plastic in their shape and function [22], and thus represent an important evolutionary innovation that contributes towards the substantial diversity and ecological versatility that characterizes this phylum. Despite the significance of arthropodization as a synapomorphy of Euarthropoda, there is a lack of consensus in terms of its precise origin among stem-lineage representatives. The phylogenetically earliest evidence of arthropodization is found among radiodonts, diverse nektobenthic stem-group euarthropods that played an important ecological role in early marine ecosystems during the early Phanerozoic [01, 04, 16, 23]. Radiodonts possess a single pair of multiarticulated and arthropodized raptorial frontal appendages that mainly served a feeding function, either for grasping, crushing, filter feeding or sediment sifting. Although some radiodonts also feature robust appendicular “gnathobase-like structures” associated with the functional head region [23], the rest

of the body consists of an unarthrodized trunk with metamericly arranged lateral body flaps for swimming [04]. By contrast, the first appearance of fully arthropodized ventral appendages remains contentious. Suggested evidence for arthropodized legs in Cambrian lobopodians [24] has been regarded as preservation artefacts caused by folding of the flexible or partially decayed cuticle [25]. Since the development of fully arthropodized biramous trunk appendages represents one of the major transitions in early euarthropod evolution [01, 02, 03, 08, 09, 13, 15, 22], resolving this issue carries direct implications for understanding the phylogenetic relationships among early representatives, as well as the emergence of one of the most versatile animal body plans during the Cambrian Explosion.

Recent studies suggest that some of the earliest branching euarthropods bore a broad carapace that covered a weakly sclerotized trunk consisting of ring-like tergites, and largely homonomous pairs of biramous appendages [01, 07, 13, 14, 15, 19]. Among this paraphyletic grade of Cambrian bivalved euarthropods, the isoxyids have been repeatedly compared with radiodonts based on the presence of a pair of raptorial frontal appendages [07, 14, 15, 19, 20]. Despite exceptional soft-tissue preservation in isoxyids including the stalked eyes and paired gut diverticulae, the detailed morphology of their body and biramous appendages remains poorly understood, generally obscured by the dorsal carapace covering the entire body [10, 11, 12, 14, 15, 17, 18, 26]. The Burgess Shale *Surusicaris* has some of the best-preserved biramous trunk appendages in isoxyids described to date [15], interpreted as weakly sclerotized and simple, annulated limbs with an elongate exopod bearing marginal setae. The trunk appendages of *Isoxys volucris* from Sirius Passet [11] show crudely preserved paddle-shaped exopods, and endopods without clear signs of segmentation. Although the presence of putative podomere boundaries has been suggested for *I. curvirostratus* and *I. auritus* from Chengjiang [12, 17], critical details of the appendicular morphology are missing in all cases to fully assess their evolutionary and ecological significance. Furthermore, whether the trunk of isoxyids was fully arthropodized or not remains completely unknown.

Here, we revise the morphology of *Isoxys* from the early Cambrian (Stage 3) Chengjiang biota in South China. We employ micro-computed tomography (micro-CT) imaging and 3D computer rendering techniques to investigate the exceptionally preserved pyritized three-dimensional organization of *Isoxys* biramous appendages, and demonstrate that isoxyids had higher degrees of morphological and functional specialization than previously considered [10, 11, 12, 14, 15, 17, 18, 26].

## Morphological description

We investigated new material of *Isoxys curvirostratus* [12] (Fig. 1; Extended Data Fig. 1–4), as well as previously published material of *Isoxys* sp. [26] (Fig. 2) from Chengjiang. *Isoxys* species share fundamental aspects of the overall morphology, including the presence of a bivalved dorsal carapace with a semicircular smooth margin, anterior and posterior cardinal spines, prominent stalked eyes and robust frontal appendages [12, 17, 26] (Figs. 1, 2). *I. curvirostratus* is distinguished by the presence of a convex dorsal carapace margin, upward bending anterior cardinal spine approximately three times longer than the posterior spine, and the presence of longitudinal striations on the posterior part of the carapace (Fig. 1; Extended Data Figs. 1–4). *Isoxys* sp. cannot be ascribed to an existing species due to the lack of

diagnostic characters such as the frontal appendages or carapace ornamentation [12, 17], and thus is treated in open nomenclature following ref. [26]. Carapace length – measured between the bases of anterior and posterior spines – ranges from 24 to 28 mm for *I. curvirostratus*, and 19 mm for *Isoxys* sp. in our studied material (Figs. 1, 2). Comparisons with previous reports on Chengjiang *Isoxys* species [12, 17, 26] suggest that our material corresponds to adults based on their size.

Soft tissues have been described for both *I. curvirostratus* and *Isoxys* sp. [12, 17, 26]. The anterior end of the body bears a pair of prominent stalked eyes with a spherical shape, and which protrude beyond the anterior carapace margin directly below the cardinal spine (Figs. 1, 2; Extended Data Figs. 1–4). The appearance of the eyes in *Isoxys* closely resembles that of the fossilized ocular structures in other Chengjiang euarthropods [2, 4, 6], consisting of a light outer layer and a dark internal mass, which likely correspond to the eye lens and pigmented retina respectively. A pair of well-developed frontal appendages is also found in close association with the stalked eyes on the anterior end of the body (Fig. 1; Extended Data Figs. 3, 4). The frontal appendages appear to attach behind the eyes, similar to *Surusicaris* [15], but their precise position within the head and relative to the mouth opening remains uncertain in our material due to the coverage by the carapace, as well as in other *Isoxys* from Chengjiang [12, 17, 26], Sirius Passet [11], Emu Bay Shale [10], and Burgess Shale [14, 18]. Our material of *I. curvirostratus* preserves the morphology of the frontal appendage in greater detail than previously described specimens [2, 12]. YKLP 16260 and YKLP 16261 shows that the frontal appendage of *I. curvirostratus* consists of six podomeres that are longer (sag.) than thick (trans.), and follows a distinctive curvature in which the ventral side is facing upwards (Fig. 1m, n). The basal podomere has a subtrapezoidal shape and lacks endites, whereas the following four podomeres are robust, subequal in length (sag.) and have distinctly curved ventral margin that bears up to a dozen spinose endites that are longer towards the podomere midline, and shorter towards the margins (Fig. 1n; Extended Data Fig. 4b). The sixth podomere is a terminal claw, of subequal length to the previous podomeres but with a slender outline. The terminal claw also bears spinose endites that are consistently short and point distally (Fig. 1o). The frontal appendages of *I. curvirostratus* are morphologically distinct from those of *I. auritus*, also known from Chengjiang [2, 17], as the latter consists of nine podomeres with a subrectangular outline, with subequal length (sag.), each bearing a single median spinose endite.

The carapace of *Isoxys* covers most of the trunk morphology in all specimens described to date [2, 10, 11, 12, 14, 17, 18, 26]. New material of *Isoxys curvirostratus* with a partially displaced carapace informs the organization of the trunk region (Fig. 1k, l; Extended Data Fig. 4a). YKLP 16261 demonstrates that the trunk of *I. curvirostratus* clearly lacks any indications of dorsal arthrodization such as well-defined tergites or epidermal segmental boundaries, despite the presence of soft tissues including the eyes, a complete biramous appendage series, and paired telson flaps on the posterior end (Fig. 1l; Extended Data Fig. 4a). The quality of preservation of YKLP 16261 featuring delicate structures such as the stalked eyes and appendages indicates that this lack of arthrodization is legitimate, rather than a taphonomic artifact caused by decay. The overall surface appearance of the biramous appendages in the studied specimens of *I. curvirostratus* and *Isoxys* sp. is comparable to those in previous reports [2, 12, 17, Fuetal2014, 26]. The appendages consist of relatively simple endopods and exopods with

setae, and appear nearly homonomous, except for a gentle increase in size from the anterior end to the middle of the body, and then decrease in size from the middle to the posterior end (Figs. 1a, l, 2a; Extended Data Fig. 3). Both *Isoxys curvirostratus* [12] and *Isoxys* sp. feature 14 pairs of ventral biramous appendages (Figs. 1, 2), which distinguish them from the 11 pairs described for the adults of *I. auritus* [17].

Micro-CT imaging and 3D rendering techniques reveal exceptional details of the pyritized limb morphology in Chengjiang fossil euarthropods that are not accessible through conventional light photography [21, 27, 28]. In *I. curvirostratus*, all the ventral appendages have a biramous construction, with the first to fourth appendage pairs being shorter and morphologically distinct from the subsequent ones (Fig. 1b–d; Extended Data Fig. 3c, d; Supplementary Videos 1, 2). The endopods have well-defined segmental boundaries expressed as regularly spaced transverse grooves along the proximodistal appendage axis. The fact that the grooves are consistent in their position within and between appendages indicates that they are not fractures in the fossil, nor a result from incomplete pyritization. The number and morphology of the endopod podomeres vary between different appendages. The shorter first to fourth biramous appendage pairs have endopods composed of at least 11 robust podomeres, each with a subtrapezoidal outline, and a strongly curved terminal claw (Figs. 1e–h, and 3c; Supplementary Videos 3–6). Each podomere carries a pair of medially located endites expressed as strong triangular spines along the ventral margin of the main limb axis (Fig. 1f–h; Supplementary Videos 4–6). The exopods of the first to fourth appendage pairs in YKLP 16260 include a slender shaft that is as long as their corresponding endopod (Fig. 1f–h; Supplementary Videos 4–6), and bear several thick paddle-shaped lamellae perpendicular to the main limb axis (Fig. 1c; Extended Data Fig. 3c, d; Supplementary Video 1). The exopod shaft also bears a terminal paddle-shaped lamella with marginal spines on its distal end (Fig. 1f; Supplementary Video 4). The anterior position of the first to fourth appendage pairs and their distinctive morphological specialization suggest that they belong to a functional six-segmented head, which also includes the segments bearing the stalked eyes and the raptorial frontal appendages. The fifth to fourteenth pairs of biramous appendages also show the preservation of fine morphological details, including endopods with at least a dozen well-defined transverse podomere boundaries, and which taper in width distally into a gently curved terminal claw (Fig. 1b, i, j; Extended Data Figs. 2a, 3b). It is likely that the full podomere count is higher, but details of the proximal portion of the appendages cannot be fully resolved. Unlike the cephalic limbs, the fifth to fourteenth pairs of biramous appendages lack endites on each podomere, but feature a pair of elongate delicate multi-articulated spines at the level of the 10<sup>th</sup> podomere (Fig. 1i, j; Extended Data Fig. 1a; Supplementary Videos 7, 8). The proximal organization of the trunk exopods in *I. curvirostratus* could not be resolved from the studied material, but the paddle-shaped lamellae are visible on the surface of specimens with well-preserved limbs such as YKLP 16260 (Fig. 1c; Supplementary Video 1).

The limb morphology of *Isoxys* sp. (Fig. 2; Supplementary Videos 9, 10) complements the findings from *I. curvirostratus* to produce a comprehensive understanding of the appendicular organization of *Isoxys*. CFM 00047 features three (rather than four) pairs of smaller biramous

appendages, and trunk endopods with more than a dozen podomeres. However, *Isoxys* sp. demonstrates that the proximal portion of the biramous appendages consists of an undifferentiated subtrapezoidal protopod (Fig. 2e, f; Supplementary Video 12). *Isoxys* sp. also shows the complete exopod organization in great detail, consisting of an elongate shaft that bears at least a dozen thick and paddle-shaped lamellae that attach perpendicular relative to the main exopod axis (Fig. 2d, f; Supplementary Video 11). The paddle-shaped lamellae imbricate with each other, and lack the fringe of short marginal setae observed in the morphologically similar exopod of Cambrian artiopods [see ref. 28]. Distally, the exopod shaft bears a single paddle-shaped lamella (Fig. 2d–f; Supplementary Videos 11, 12), as also observed in *I. curvirostratus* (Fig. 1e; Supplementary Video 3). CFM 00047 demonstrates that the imbrication of the paddle-shaped lamellae in the exopod can produce an appearance akin to cuticular folds on the surface of the fossils (Fig. 1l) [15, 25], which has led to previous misinterpretations of the biramous appendage structure.

### Appendage differentiation in *Isoxys*

New material and the use of micro-CT imaging and 3D rendering techniques to detect the iron-enriched non-biomineralized morphology in pyritized Chengjiang fossils reveal new details of the anatomical organization in *Isoxys* (Fig. 3a–d), with direct implications for its palaeoecological and evolutionary significance. The robust frontal appendages in *Isoxys curvirostratus* are well suited for a raptorial grasping function following an upwards stroke in front of the carapace (Fig. 3b), which combined with the presence of prominent anterior-facing stalked eyes indicates that this bivalved euarthropod was an active visual predator [10, 12, 14, 26, 29]. The presence of a short unarthrodized trunk concealed within the carapace suggests that this body region was not efficient for swimming on its own, as it lacks the rigid muscle attachment sites needed for propulsion as observed in other Cambrian bivalved forms with cylindrical abdominal tergites [07, 13, 20, 27]. Instead, swimming in *Isoxys* was most likely achieved by the rhythmic movement of the biramous appendages powered by the paddle-shaped lamellae on the exopods [26, 29] (Fig. 3). The arthropodized trunk endopods would allow walking on the benthos. Whereas the raptorial frontal appendages are well equipped for prey capture thanks to the substantial spinose armature observed in *I. curvirostratus* (Fig. 1m–o), the following biramous appendages indicate a further degree of functional differentiation. We demonstrate that the four anteriormost biramous appendages of *I. curvirostratus* are not only shorter, but that their endopods bear robust endites and a strongly curved terminal claw (*contra* ref. 02, 10, 12, 14, 15, 26) (Fig. 2e–h). The integration of the four biramous appendage pairs into a functionally specialized head region suggest that they were used for processing soft-bodied food items drawn into the anterior space within the carapace – once grasped by the frontal appendages – before consumption. By contrast, the undifferentiated protopod and absence of spinose endites on the trunk biramous appendage pairs – as observed in *Isoxys* sp. – suggest that they were not used for feeding, but instead were restricted to locomotion for either swimming vertically in the water column [29] or walking on the benthos. The paired slender and multiarticulated spines on the 10<sup>th</sup> podomere of the trunk endopods are too delicate for food processing; we hypothesize they might have a sensorial function or provide some mechanical support during benthic locomotion. The lack of

adaptations for feeding on the trunk biramous appendage pairs also argues against a scavenging or detritivorous diet, as these strategies generally require a dense proximal enditic armature that forms a median food groove for processing organic matter [21, 28]. These findings indicate that the biramous appendages of *Isoxys* possessed a higher degree of heteronomy and functional differentiation than previously considered [01, 10, 12, 14], and reveal an unexpected complexity in the feeding ecology of pelagic predators in early marine ecosystems [26, 29].

## Implications of early euarthropod evolution

*Isoxys curvirostratus* uniquely combines the presence of fully arthropodized biramous appendages, a morphologically and functionally specialized six-segmented head, and lack of trunk arthrodization (Figs. 3, 4), all of which are critical characters for reconstructing early euarthropod evolution [01, 02, 08, 13]. Notably, *I. curvirostratus* and *Isoxys* sp. demonstrate that all the biramous appendages share similarities with those of deuteropods in a more crown-wards phylogenetic position [08]. The multi-podomorous endopods of *Isoxys* are comparable to those of other Cambrian bivalved euarthropods [17, 20] and fuxianhuiids [06], suggesting that they could reflect the ancestral organization of the earliest arthropodized limbs. Similarly, the slender exopod shaft with paddle-shaped lamellae has recently been recognized in a number of Cambrian artiopods, and suggested as potentially symplesiomorphic for that clade [28]. The Burgess Shale *Surusicaris* also has three anteriormost differentiated ventral appendages [15], indicating that the presence of a multi-segmented head region is widespread among isoxyids. Critically, an isoxyid-like cephalization pattern has been recently recognized in the early diverging stem-group euarthropod *Kylinxia* from Chengjiang [02], which strikingly also possesses upwards-facing raptorial frontal appendages and four pairs of smaller biramous appendages in the head. *Isoxys* and *Kylinxia* also share the presence of paired telson flaps, although other aspects of their body morphology differ substantially, such as the presence of trunk tergites and absence of a carapace in the latter. Indeed, the lack of trunk arthrodization in *Isoxys* is comparable with the absence of epidermal dorsal segmentation observed in radiodonts [03, 23, 30], which suggests that *Isoxys* embodies an earlier step in the evolutionary history of the euarthropod body plan relative to the fully arthropodized *Kylinxia*.

The results of phylogenetic analyses using maximum parsimony and Bayesian inference (Fig. 3e–g; Extended Data Figs. 5–7) to explore the evolutionary implications of our new morphological data provide support for the hypothesis that *Isoxys* may be the outgroup to other deuteropods, rather than *Kylinxia* (*contra* ref. 02). The maximum parsimony analysis with implied weights (Fig. 3e; Extended Data Fig. 5a) resolves isoxyids as a paraphyletic grade and the earliest branching members of Deuteropoda, and *Kylinxia* as a stem-group chelicerate, while equal weights maintain *Kylinxia* as the outgroup of Deuteropoda in all parsimonious trees (Fig. 3f; Extended Data Fig. 5b). These results carry different evolutionary implications. Under the *Isoxys*-first scenario, the arthropodized ventral appendages have a single origin at the base of Deuteropoda, and trunk arthrodization is a synapomorphy of crown-group Euarthropoda (Fig. 3e). The *Kylinxia*-first scenario also supports a single origin for arthropodized ventral appendages, but requires the repeated evolution of trunk arthrodization in *Kylinxia*, its loss among isoxyids, and reappearance in crown-group Euarthropoda (Fig. 3f). Thus, *Isoxys*-first represents the most

parsimonious hypothesis for the origin of arthropodization and arthroization within the euarthropod stem lineage from a character transformation perspective.

Bayesian inference supports *Kylinxia* as the outgroup of Deuteropoda and the monophyly of isoxyids (Fig. 3g; Extended Data Fig. 5c). This result provides two equally parsimonious scenarios of character evolution: either a single origin for trunk arthroization in Deuteropoda (evidenced by *Kylinxia*) with secondary loss among monophyletic isoxyids, or the repeated evolution of trunk arthroization in *Kylinxia* and crown-group Euarthropoda. Although *Kylinxia* as the outgroup has a posterior probability of 0.78 (Fig. 3g; Extended Data Fig. 5c), we use treespace analysis [30] to visualize the topologies retrieved by our phylogenetic reconstruction ( $n = 2317$  trees total), and the degree of uncertainty at this node, information that is omitted when viewing a consensus tree alone. Indeed, 20% ( $n = 464$  trees) of the retrieved topologies support isoxyids as the outgroup, a relationship that occupies a comparable amount of treespace as does the alternative *Kylinxia* despite being visited fewer times by the Markov chains (Fig. 3h; Extended Data Fig. 6). This implies that isoxyids as the outgroup are plausible given the morphological data available. Similar to the results of experiments by ref. 02, removal of *Kylinxia* from the morphological dataset completely supports paraphyletic isoxyids as the outgroup of all other deuteropods (Extended Data Fig. 7). In this context, it appears that the unique morphology of *Kylinxia* may be responsible for character conflict within the euarthropod stem lineage. Ultimately, our results provide evidence that isoxyids are viable candidates as the earliest branching members of Deuteropoda. The reinvigorated understanding of the body organization of *Isoxys* made possible by new fossil material and micro-CT imaging consolidates their key role in the step-wise evolution of the fundamental exoskeletal characters that define crown-group Euarthropoda.

## Online content

Any methods, additional references, Nature Research Reporting summary, source data, supplementary information, peer review information; details of author contributions and competing interests; and statements of date and code availability are available at TBC.

## Declarations

**Acknowledgements.** We thank Mr. Hong Liu (Kunming, China) for collecting the specimen YKLP 16261, and Prof. Dr. Roland Melzer (München, Germany) for detecting the signal/noise ratio of YKLP 16260.

**Author contributions.** XGH, DYZ and JG collected all fossils except YKLP 16261. HJM scanned all fossils. DYZ, YL and JOH designed the research. CXZ processed micro-CT data. CXZ and JOH prepared the figures with input from all co-authors. JMW designed and performed the phylogenetic analysis with input from JOH. CXZ, DYZ, JOH, JMW and YL wrote the manuscript with input from all co-authors. All authors discussed and approved the manuscript.

**Competing interests.** The authors declare no competing interests.

**Funding:** This study is supported by grants YNWR-QNBJ-2019-295, 2019DG050, 2018FA025, and 2015HC029 from the Yunnan Provincial Science and Technology Department, grant 41861134032 from the National Natural Science Foundation of China, and grant 201905 from the Institute of Geology of Geophysics, Chinese Academy of Sciences, and the Harvard China Fund. JMW was supported by National Science Foundation DEB #1856679.

## References

1. Edgecombe, G.D., 2020. Arthropod Origins: Integrating Paleontological and Molecular Evidence. *Annual Review of Ecology, Evolution, and Systematics*, 51, pp.1-25.
2. Zeng, H., Zhao, F., Niu, K., Zhu, M. and Huang, D., 2020. An early Cambrian euarthropod with radiodont-like raptorial appendages. *Nature*, 588(7836), pp.101-105.
3. Budd, G.E. and Daley, A.C., 2012. The lobes and lobopods of *Opabinia regalis* from the middle Cambrian Burgess Shale. *Lethaia*, 45(1), pp.83-95.
4. Cong, P., Ma, X., Hou, X., Edgecombe, G.D. and Strausfeld, N.J., 2014. Brain structure resolves the segmental affinity of anomalocaridid appendages. *Nature*, 513(7519), pp.538-542.
5. Park, T.Y.S., Kihm, J.H., Woo, J., Park, C., Lee, W.Y., Smith, M.P., Harper, D.A., Young, F., Nielsen, A.T. and Vinther, J., 2018. Brain and eyes of *Kerygmachela* reveal protocerebral ancestry of the panarthropod head. *Nature communications*, 9(1), pp.1-7.
6. Yang, J., Ortega-Hernández, J., Butterfield, N.J. and Zhang, X.G., 2013. Specialized appendages in fuxianhuiids and the head organization of early euarthropods. *Nature*, 494(7438), pp.468-471.
7. Aria, C. and Caron, J.B., 2017. Burgess Shale fossils illustrate the origin of the mandibulate body plan. *Nature*, 545(7652), pp.89-92.
8. Ortega-Hernández, J., 2016. Making sense of 'lower' and 'upper' stem-group Euarthropoda, with comments on the strict use of the name Arthropoda von Siebold, 1848. *Biological Reviews*, 91(1), pp.255-273.
9. Budd, G.E., 2002. A palaeontological solution to the arthropod head problem. *Nature*, 417(6886), pp.271-275.
10. García-Bellido, D.C., Paterson, J.R., Edgecombe, G.D., Jago, J.B., Gehling, J.G. and Lee, M.S., 2009. The bivalved arthropods *Isoxys* and *Tuzoia* with soft-part preservation from the Lower Cambrian Emu Bay Shale Lagerstätte (Kangaroo Island, Australia). *Palaeontology*, 52(6), pp.1221-1241.
11. Stein, M., Peel, J.S., Siveter, D.J. and Williams, M., 2010. *Isoxys* (Arthropoda) with preserved soft anatomy from the Sirius Passet Lagerstätte, lower Cambrian of North Greenland. *Lethaia*, 43(2), pp.258-265.
12. Fu, D.J., Zhang, X.L. and Shu, D.G., 2011. Soft anatomy of the Early Cambrian arthropod *Isoxys curvirostratus* from the Chengjiang biota of South China with a discussion on the origination of great appendages. *Acta Palaeontologica Polonica*, 56(4), pp.843-852.

13. Legg, D.A., Sutton, M.D., Edgecombe, G.D. and Caron, J.B., 2012. Cambrian bivalved arthropod reveals origin of arthropodization. *Proceedings of the Royal Society B: Biological Sciences*, 279(1748), pp.4699-4704.
14. Legg, D.A. and Vannier, J., 2013. The affinities of the cosmopolitan arthropod *Isoxys* and its implications for the origin of arthropods. *Lethaia*, 46(4), pp.540-550.
15. Aria, C. and Caron, J.B., 2015. Cephalic and limb anatomy of a new isoxyid from the Burgess Shale and the role of “stem bivalved arthropods” in the disparity of the frontalmost appendage. *PloS one*, 10(6), p.e0124979.
16. Lerosey-Aubril, R., Kimmig, J., Pates, S., Skabelund, J., Weug, A. and Ortega-Hernández, J., 2020. New exceptionally preserved panarthropods from the Drumian Wheeler Konservat-Lagerstätte of the House Range of Utah. *Papers in Palaeontology*, 6(4), pp.501-531.
17. Fu, D., Zhang, X., Budd, G.E., Liu, W. and Pan, X., 2014. Ontogeny and dimorphism of *Isoxys auritus* (Arthropoda) from the early Cambrian Chengjiang biota, South China. *Gondwana Research*, 25(3), pp.975-982.
18. Vannier, J., García-Bellido, D.C., Hu, S.X. and Chen, A.L., 2009. Arthropod visual predators in the early pelagic ecosystem: evidence from the Burgess Shale and Chengjiang biotas. *Proceedings of the Royal Society B: Biological Sciences*, 276(1667), pp.2567-2574.
19. Legg, D.A., Sutton, M.D. and Edgecombe, G.D., 2013. Arthropod fossil data increase congruence of morphological and molecular phylogenies. *Nature communications*, 4(1), pp.1-7.
20. Legg, D.A. and Caron, J.B., 2014. New Middle Cambrian bivalved arthropods from the Burgess Shale (British Columbia, Canada). *Palaeontology*, 57(4), pp.691-711.
21. Zhai, D., Edgecombe, G.D., Bond, A.D., Mai, H., Hou, X. and Liu, Y., 2019. Fine-scale appendage structure of the Cambrian trilobitormorph *Naraoia spinosa* and its ontogenetic and ecological implications. *Proceedings of the Royal Society B*, 286(1916), p.20192371.
22. Boxshall, G.A., 2004. The evolution of arthropod limbs. *Biological Reviews*, 79(2), pp.253-300.
23. Cong, P.Y., Edgecombe, G.D., Daley, A.C., Guo, J., Pates, S. and Hou, X.G., 2018. New radiodonts with gnathobase-like structures from the Cambrian Chengjiang biota and implications for the systematics of Radiodonta. *Papers in Palaeontology*, 4(4), pp.605-621.
24. Liu, J., Steiner, M., Dunlop, J.A., Keupp, H., Shu, D., Ou, Q., Han, J., Zhang, Z. and Zhang, X., 2011. An armoured Cambrian lobopodian from China with arthropod-like appendages. *Nature*, 470(7335), pp.526-530.
25. Ma, X., Edgecombe, G.D., Legg, D.A. and Hou, X., 2014. The morphology and phylogenetic position of the Cambrian lobopodian *Diania cactiformis*. *Journal of Systematic Palaeontology*, 12(4), pp.445-457.
26. Vannier, J., García-Bellido, D.C., Hu, S.X. and Chen, A.L., 2009. Arthropod visual predators in the early pelagic ecosystem: evidence from the Burgess Shale and Chengjiang biotas. *Proceedings of the Royal Society B: Biological Sciences*, 276(1667), pp.2567-2574.

27. Zhai, D., Ortega-Hernández, J., Wolfe, J.M., Hou, X., Cao, C. and Liu, Y., 2019. Three-dimensionally preserved appendages in an early Cambrian stem-group pancrustacean. *Current Biology*, 29(1), pp.171-177.
28. Schmidt, M., Hou, X.G., Belojevic, J., Zhai, D., Mai, J., Melzer, R.R., Ortega-Hernández, J., and Liu Y. Before trilobite legs: *Pygmaclypeatus daziensis* reconsidered and the ancestral appendicular organization of Cambrian artiopods. *bioRxiv* (doi: 10.1101/2021.08.18.456779)
29. Pates, S., Daley, A.C., Legg, D.A., and Rahman, I.A. 2021. Vertically migrating *Isoxys* and the early Cambrian biological pump. *Proceedings of the Royal Society B*, 288: 20210464.
30. Pates, S., Wolfe, J. M., Lerosey-Aubril, R., Daley, A. C., & Ortega-Hernández, J. (2021). New opabiniid diversifies the weirdest wonders of the euarthropod lower stem group. *BioRxiv*. Doi: 10.1101/2021.03.10.434726

## Methods

### Material

All studied specimens were collected from the mudstones in the Cambrian Stage 3 Yu'an-shan Member of the Chiungchussu Formation. The specimens YKLP 16260–16264 were collected from the Haikou area of Kunming, China, and are housed at the Yunnan Key Laboratory for Palaeobiology, Yunnan University. Specimen CFM 00047 was collected from the Xiaolantian section in Chengjiang, and is housed at the Chengjiang Fossil Museum, Yuxi.

### Fossil imaging

Fossil specimens were photographed with a Keyence VHX 6000 stereomicroscope. In order to observe the structures buried within the rock matrix and to produce three-dimensional models of the preserved morphology, micro-computed tomography imaging and 3D computer rendering techniques were applied. The best outcome is from specimens YKLP 16260 and CFM 00047. Specimen YKLP 16260 was first scanned with a GE Phoenix Nanotom cone beam scanner at the Bavarian State Collection of Zoology, Bavarian Natural History Collections, München, Germany, to detect the signal/noise ratio, and then with a Zeiss Xradia 520 Versa X-ray microscope at the YKLP to obtain images with higher resolutions. For the Xradia 520 Versa scanning, the energy and the resolution were set at 60 kv/5w and 15.25 µm for slab a, and at 60 kv/5w and 15.89 µm, 50 kv/4w and 8.48 µm for slab b (scanned twice), to obtain a higher resolution of the anterior part of the body. Specimen CFM 0047 was scanned with a Zeiss Xradia 520 Versa X-ray microscope with the above two parameters set at 70 kv/6w and 5.41 µm for overview scanning, and at 60 kv/5w and 11.6 µm for small-field, detailed scanning.

### Phylogenetic analysis

To assess the phylogenetic position of *Isoxys*, we re-analyzed the published morphological matrix of ref [02]. We recoded *Isoxys curvirostratus*, and edited codings of other isoxyid taxa, according to new

anatomical data herein. We removed characters 114, 202, and 280 as they represented taphonomic artefacts based on more recent interpretations. Therefore, the matrix comprised 81 taxa and 280 discrete characters. Details of all characters including character descriptions and scorings may be downloaded from MorphoBank [31] ([www.morphobank.org](http://www.morphobank.org), reviewer login 'email address': 4030, reviewer password: isoxys).

We analyzed this morphological dataset in MrBayes v.3.2.7 [32], implementing the Mk model of character evolution [33] with gamma distributed among-character rate variation for four runs of four chains and 10 million generations, with 25% burnin. Convergence was assessed based on standard deviations of split frequencies  $< 0.01$ , reaching effective sample size  $>200$  for every parameter, and by comparing posterior distributions in Tracer v.1.7.1 [34]. We also analyzed the morphological matrix using maximum parsimony in TNT v.1.5 [35] using both equal weights and implied weights ( $k = 3$ ). For both weighting schemes, we required the shortest tree to be retrieved 100 times, and used tree bisection-reconnection to swap one branch at a time on the trees in memory.

We further interrogated support for alternative phylogenetic positions of isoxyiids using treespace visualization [36, 37, 30]. As described in ref. [30], this method calculates pairwise unweighted Robinson-Foulds (RF) distances for the total set of unrooted trees (Bayesian and maximum parsimony) using *phangorn* v.2.5.5 [38] and visualizes the RF distances using classical multidimensional scaling in *ape* v.5.3 [39]. See ref. [30] for additional details of the method.

## Preservation

Like most other fossils of *Isoxys*, the specimens studied herein (Figs. 1, 2, and Extended Data Figs. 1–4) are laterally compressed, although the small offset between the appendages from left and right sides in the specimen YKLP 16260 (and Extended Data Fig. 2c, e; Supplementary Videos 10, 12) indicates an oblique-lateral orientation for the ventral appendages. Whereas most of the soft-tissue morphology is encased within the carapace, the stalked eyes, frontal appendages, the distal parts of the trunk appendages, and the posterior end of the telson usually extend beyond the carapace margins. In YKLP 16261 (Fig. 2a), the posterior part of the body was partially disarticulated from the carapace, revealing the trunk organization. Specimens YKLP 16260 and CFM 00047 (Figs. 1, 2) show a strong degree of pyritization, generating a density contrast with the rock matrix that facilitates micro-CT imaging of exceptionally preserved structures.

## Reporting summary

Further information on research design is available in the Nature Research Reporting Summary linked to this paper.

## Data availability

All data analysed in this paper are available as part of the Article, Extended Data Figures 1–7 or Supplementary Information. Original tomographic datasets are available on Dryad (<https://doi.org/xxxx>)

as grayscale TIFF images, and are freely accessible for visualization. Phylogenetic results are available at the same Dryad link, while the detailed morphological matrix is available at MorphoBank ([www.morphobank.org](http://www.morphobank.org), reviewer login ('email address'): 4030, reviewer password: opabiniids). Publicly accessible versions of the tomographic models in Figures 1 and 2 are hosted in Sketchfab at the hyperlink TBC.

## Methods References

31. M. A. O'Leary, S. G. Kaufman, Morphobank 3.0: Web application for morphological phylogenetics and taxonomy (2012), (available at <http://www.morphobank.org>).
32. Ronquist, F., Teslenko, M., Van Der Mark, P., Ayres, D.L., Darling, A., Höhna, S., Larget, B., Liu, L., Suchard, M.A. and Huelsenbeck, J.P., 2012. MrBayes 3.2: efficient Bayesian phylogenetic inference and model choice across a large model space. *Systematic biology*, 61(3), pp.539-542.
33. Lewis, Paul O. "A likelihood approach to estimating phylogeny from discrete morphological character data." *Systematic biology* 50.6 (2001): 913-925.
34. A. Rambaut, A. J. Drummond, D. Xie, G. Baele, M. A. Suchard, Posterior summarization in Bayesian phylogenetics using Tracer 1.7. *Syst. Biol.* **67**, 901–904 (2018).
35. Goloboff, P. A. and Catalano, S. A. (2016) 'TNT version 1.5 including a full implementation of phylogenetic morphometrics', *Cladistics*, 32, pp. 221–238.
36. D. M. Hillis, T. A. Heath, K. St. John, Analysis and visualization of tree space. *Syst. Biol.* **54**, 471–482 (2005).
37. A. M. Wright, G. T. Lloyd, Bayesian analyses in phylogenetic palaeontology: interpreting the posterior sample. *Palaeontology*. **63**, 997–1006 (2020).
38. K. P. Schliep, phangorn: Phylogenetic analysis in R. *Bioinformatics*. **27**, 592–593 (2011).
39. E. Paradis, K. Schliep, Ape 5.0: An environment for modern phylogenetics and evolutionary analyses in R. *Bioinformatics*. **35**, 526–528 (2019).

## Figures

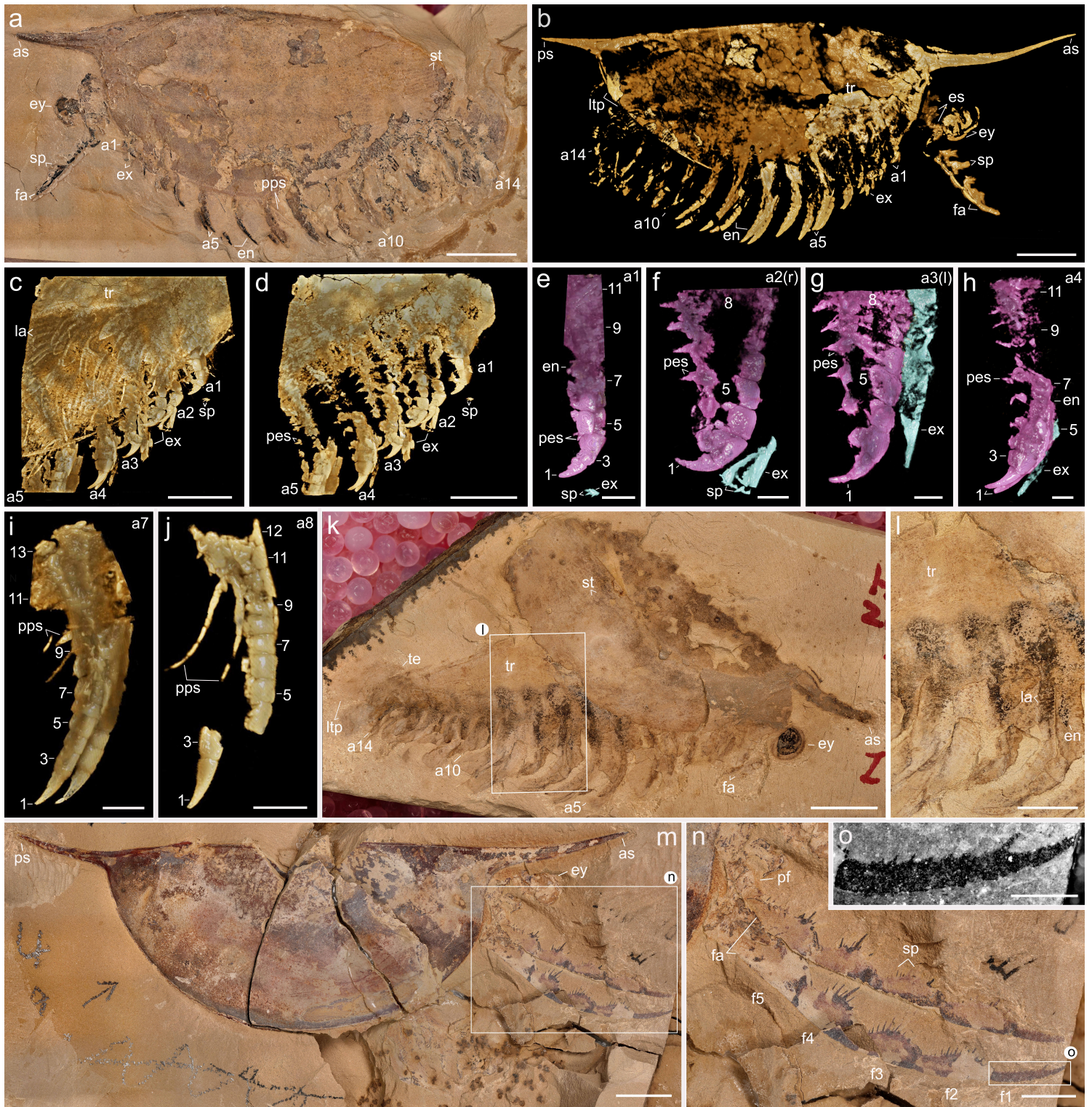


**Figure 1**

Trunk and appendage morphology of *Isoxys curvirostratus* from the early Cambrian (Stage 3) Chengjiang in South China. a–j, YKLP 16260. a, Complete specimen of *Isoxys curvirostratus* photographed under reflected light. b, Tomographic model of complete specimen in lateral view. c, Detail of tomographic model showing anterior trunk region in lateral view. d, Anterior trunk region with carapace digitally removed. e, Tomographic model of isolated first trunk appendage pair in lateral view showing morphology of endopod (purple) and exopod (blue). f, Tomographic model of second appendage pair in

ventral view. g, Tomographic model of isolated third appendage pair in ventral view. h, Tomographic model of fourth appendage pair in ventral view. i, Tomographic model of seventh appendage pair in lateral view. j, Tomographic model of eighth appendage pair in lateral view, showing presence of elongate multi-articulated spines. k, l, YKLP 16261a. k, complete specimen of *Isoxys curvirostratus* photographed under reflected light, showing partially disarticulated carapace and unarthrodized trunk. l, magnification of unarthrodized trunk and paddle-shaped lamellae in exopod. m–o, YKLP 16266. m, Complete specimen of *Isoxys* cf. *curvirostratus* with well-preserved frontal appendages photographed under reflected light. n, Detail of raptorial frontal appendages. o, Detail of elongate terminal claw showing short endites. Abbreviations: an, the nth ventral appendage; as, anterior spine; en, endopod; es, eye stalk; ex, exopod; ey, eye; fa, frontal appendage; fn, podomeres of the frontal appendage from the distal to proximal; la, lamellae of exopod; ltp, lateral processes of telson; pes, the paired spines on each endite; pf, proximal part of the frontal appendage; pps, paired posterior spines on endopod; ps, posterior cardinal spine of carapace; sp, spines; st, striated ornament; te, telson; tr, trunk. Numbers indicate endopod podomeres. Scale bars: a, b, k, m, 5 mm; c, d, 2.5 mm; e, 1 mm; f–h, 0.5 mm; i, j, o, 1 mm.

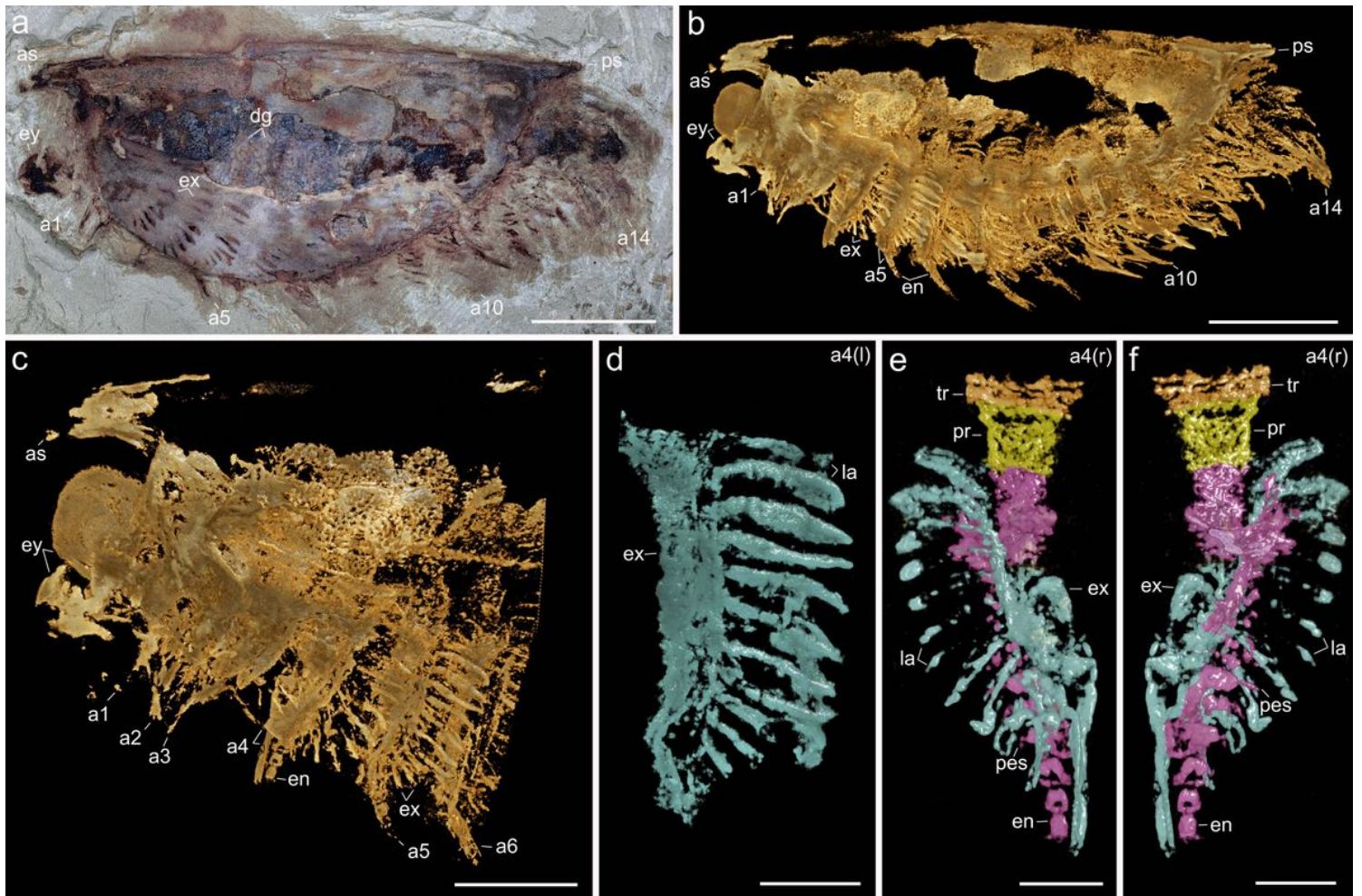


**Figure 2**

Appendicular morphology of *Isoxys* sp. from the early Cambrian (Stage 3) Chengjiang in South China. a, CFM 00047, complete specimen photographed under reflected light. b, Tomographic model of complete specimen in lateral view. c, Tomographic model showing magnification of anterior body in lateral view

with well-preserved appendages. d, Tomographic model of isolated exopod from left fourth appendage in lateral view showing elongate shaft and paddle-shaped lamellae. e, Tomographic model of exopod from right fourth appendage pair in lateral view showing protopod (yellow), endopod (purple) and exopod (blue). f, Tomographic model of exopod from right fourth appendage pair in lateral view, rotated 180 degrees. Abbreviations: an, the nth ventral appendage; as, anterior spine; dg, digestive gland; en, endopod; ey, eye; la, lamellae of exopod; pr, protopod; ps, posterior cardinal spine of carapace; tr, trunk. Numbers indicate endopod podomeres. Scale bars: a, b, 5 mm; c, 2.5 mm; d–f, 1 mm.

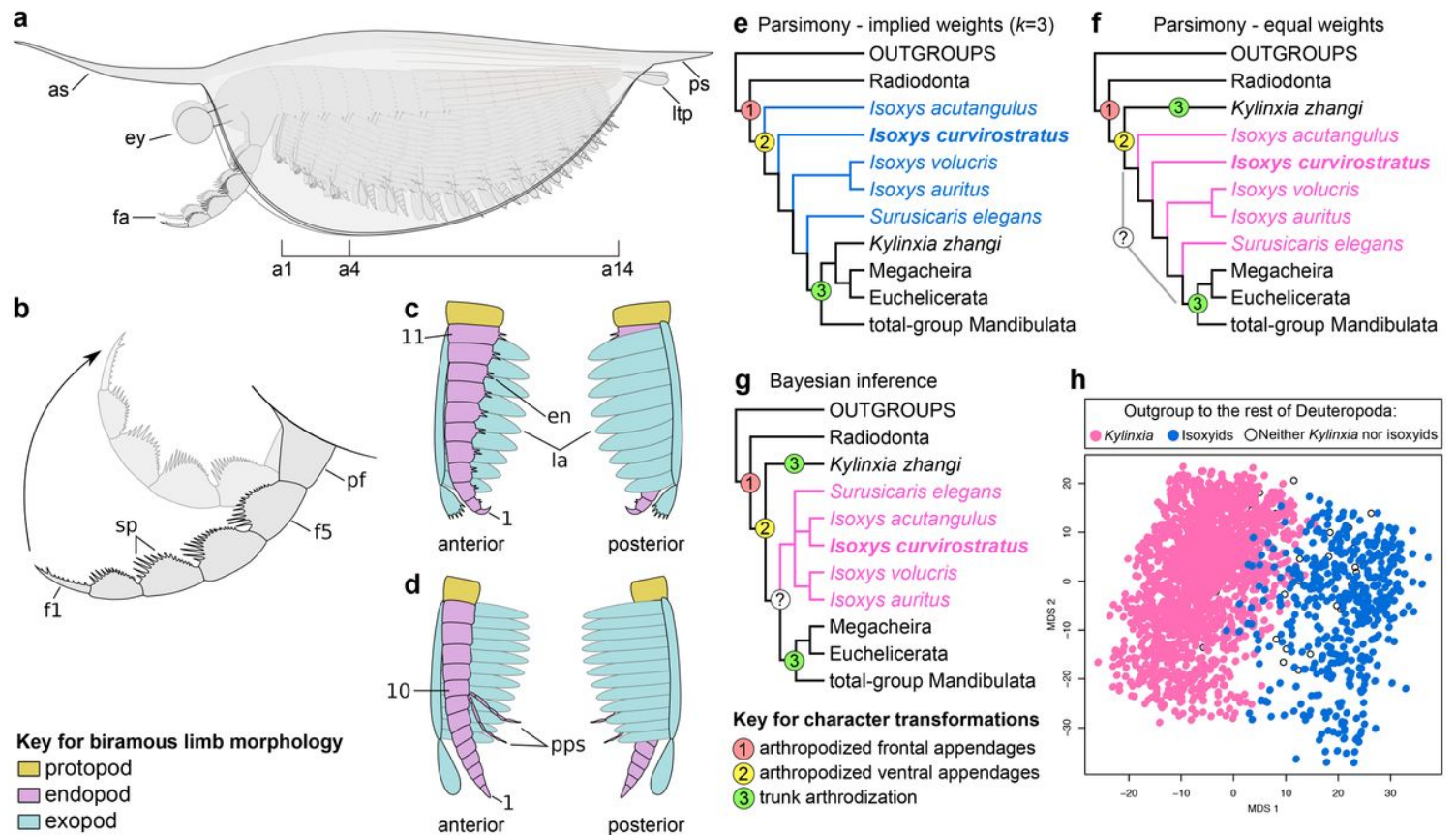


**Figure 3**

Morphological reconstruction and phylogenetic position of *Isoxys curvirostratus*. a, Lateral view. b, Detail of the frontal appendage. c, Morphology of anterior batch of biramous appendages (a1–a4). d, Morphology of posterior batch of biramous appendages (a5–a14). e. Simplified strict consensus of maximum parsimony under implied weights (1 MPT, 699 steps, CI: 0.496, RI: 0.866). f. Simplified strict consensus of maximum parsimony under equal weights (12 MPTs, 705 steps, CI: 0.492, RI: 0.864). g. Majority rule consensus tree retrieved with Bayesian inference. h. Treespace analysis comparing the distribution of topologies favoring isoxyids versus *Kylinxia* as the outgroup to other deuteropods. See Extended Data Figs. 5 and 6 for detailed results and support values. Abbreviations: an, the nth ventral appendage; as, anterior spine; en, endopod; ey, eye; fa, frontal appendage; fn, podomeres of the frontal appendage from the distal to proximal; la, lamellae of exopod; pf, proximal part of the frontal appendage; ps, posterior cardinal spine of carapace; pps, paired posterior spines on endopod; sp, spines. Numbers indicate endopod podomeres.

## Supplementary Files

This is a list of supplementary files associated with this preprint. Click to download.

- [ExtendedDataFigure1reduced.jpg](#)
- [ExtendedDataFigure2reduced.jpg](#)
- [ExtendedDataFigure3reduced.jpg](#)
- [ExtendedDataFigure4reduced.jpg](#)
- [ExtendedDataFigure5.png](#)
- [ExtendedDataFigure6.png](#)
- [ExtendedDataFigure7.png](#)
- [videoofFig.1c.mp4](#)
- [videoofFig.1d.mp4](#)
- [videoofFig.1e.mp4](#)
- [videoofFig.1f.mp4](#)
- [videoofFig.1g.mp4](#)
- [videoofFig.1h.mp4](#)
- [videoofFig.1i.mp4](#)
- [videoofFig.1j.mp4](#)
- [videoofFig.2b.mp4](#)
- [videoofFig.2c.mp4](#)
- [videoofFig.2d.mp4](#)
- [videoofFig.2e.mp4](#)